Flow-based path planning for multiple homogenous UAVs for outdoor formation-flying

Mahmud Suhaimi Ibrahim System Engineer mutashi@gmail.com Shantanu Rahman Software Engineer rahmanshantanu69@gmail.com Muhammad Samin Hasan Chief Research Officer muhammadsaminhasan@gmail.com

Minhaj Uddin Ahmad System Engineer minhajuddin@iut-dhaka.edu Abdullah Abrar Software Engineer abdullahabrar@iut-dhaka.edu

Abstract—Collision-free path planning is the most crucial component in multi-UAV formation-flying (MFF). We use unlabeled homogenous quadcopters (UAVs) to demonstrate the use of a flow network to create complete (inter-UAV) collision-free paths. This procedure has three main parts: 1) Creating a flow network graph from physical GPS coordinates, 2) Finding a path of minimum cost (least distance) using any graph-based path-finding algorithm, and 3) Implementing the Ford-Fulkerson Method to find the paths with the maximum flow (no collision). Simulations of up to 64 UAVs were conducted for various formations, followed by a practical experiment with 3 quadcopters for testing physical plausibility and feasibility. The results of these tests show the efficacy of this method's ability to produce safe, collision-free paths.

Index Terms—collision-free paths, flow-network graph, maximum flow, Ford-Fulkerson algorithm

I. INTRODUCTION

Multi-UAV path planning problems arise in various fields, including but not limited to, agriculture [1], inspection [2], [3], entertainment [4], and military applications [5]. The issue boils down to a group of UAVs trying to traverse from a set of initial locations to a set of goal locations without colliding with each other or environmental obstacles. For specific applications like outdoor multi-UAV formation flying (MFF), the UAVs need to form a certain shape. Often, in these cases, the UAVs do not need to be labeled. Meaning that the goal locations of the UAVs are independent from their identity.

A broad range of algorithms for multi-UAV path planning are available at the moment. We do not classify all of these approaches in this paper because our methodology as a whole does not fall into any pre-existing categories. An extensive summary of work and research on collision-free path-planning algorithms that exist to this day can be found in [6] and [7]. Having said that, we do provide a brief overview of a few methods and their limitations if they were to be used as standalone algorithms for collision-free path planning.

The classical path-finding methods such as A* in [8], RRT* in [9] and their variations for single UAVs have been

The authors of this work are employees of ANTS Aerial Systems Ltd, based in Dhaka, Bangladesh. This paper is an outcome of a drone light show project developed by the company.

repurposed to work with multiple UAV systems. The main problem with these algorithms is that they do not have a collision avoidance system. The generated paths may overlap, and the speed of the UAVs would, in that case, need to be varied to avoid collisions. Nevertheless, their output could be used as an initiator for the Ford-Fulkerson Algorithm.

Potential field algorithms emulate a field of energy where low-energy areas indicate lower chances of collision [10], [11]. These approaches are useful in certain small, controlled spaces, but in a large and complex environment, they do not guarantee a complete solution. Improved variations of such techniques can be found in [12] with the Fast-Marching Square algorithm. These are still sub-optimal and will fail to find the solution in some instances.

Graph Neural Networks (GNN), another heavily researched method for multi-UAV path planning, is an extension of Convolutional Neural Networks (CNN) for graph data. To implement GNN, the path planning problem has to be formulated as a sequential decision-making problem. At every instant, each UAV takes an action with the objective of reaching its destination [13]. It also requires the UAVs to constantly communicate with each other while traveling. This method allows the robots to have a certain level of autonomy and may not require mapping of the region to function. However, the drawback is that the computational complexity and cost of this method are high. Beyond the cost, there is no guarantee that it will reach the destination, which in cases of emergency response or light shows may be catastrophic [14].

Another more recent approach is to reinterpret the problem as a linear programming problem (LPP). This method is effective in a wide range of applications, but it is most commonly used in operations research or computer science. It might, however, just as readily be utilized for path planning. For example, [15] and [16] interpret the paths of multiple robots as flows in a flow network, which in essence is an LPP problem [17]. Their solution, however, is limited to ground-based robots in a 2D environment.

Our approach extends the idea of using flow networks for path planning to aerial vehicles in an outdoor space; a 3D environment. It involves a process composed of several stages that utilize certain existing solutions and implement a few novel techniques. To show the robustness of our technique we have both simulated extreme collision-prone cases with numerous UAVs and conducted a practical experiment with quadcopters in an outdoor environment.

The rest of the paper is divided into four sections. Section II describes the methodology and the theory behind our approach, followed by Section III, which gives detailed information about the components used for experimentation. Section IV is dedicated to the results and discussion of all the simulations and practical tests. Finally, Section V is a brief summary of the work and possible future improvements.

II. METHODOLOGY

Our approach to finding paths for a multi-UAV system involves two steps. First, we model the physical space as a flow network. A flow network is a directed graph where each edge has a capacity and receives a flow. Then we use an algorithm known as the Ford-Fulkerson algorithm to find the paths that provide maximum flow to the network.

A. Directed Weighted Graphs

A directed weighted graph, G=(V,E), is composed of a set of *vertices (nodes)*, V, which are connected by a set of directed weighted *edges*, E. For a pair of nodes $u,v\in V$, an edge $e=(u,v,w)\in E$, represents a connection from u to v with a weight, w. Concepts of *flow* and the *capacity* of an edge will be discussed in section II-C.

B. Bellman-Ford Algorithm

The Bellman Ford Algorithm is a graph-based path-finding algorithm for finding the shortest path between a pair of nodes in a directed weighted graph. The starting node is called a source node, and the destination node is called the sink node. Bellman-Ford incrementally finds the shortest path between these two nodes. For any graph, G = (V, E), let us define dis[v], which is a mapping from v to a number which is the cost of the shortest path available till now, and from[v], which is also a mapping from v to another vertex, which tells us from which v was updated. We consider the outgoing edges of each vertex. It is trivial that, for any edge(u, v, w), dis[v] =min(dis[v], dis[u] + w), where the dis[v] value is updated for any edge we set from[v] = u. This procedure is called incremental path relaxation. The procedure is repeated n-1times, where n is the number of nodes. Backtracking the *sink* node using flow mapping will give us the path of minimum cost from the source to the sink. Thus, a path is generated between the source and the sink.

C. Flow Network and Maximum Flow Problem

A Flow network is a Directed Weighted Graph with some extra properties. The flow of an edge in a graph, f(e), is a quantity that can represent various things depending on the situation. Our paper represents the number of UAVs that travel through an edge as flow. With that, we also have the capacity, C(e), which is the maximum amount of flow allowed through an edge. Additionally, we define two special nodes:

- The *source* node, s, which provides an infinite amount of flow and does not have any input edges.
- The sink node, t, which takes in an infinite amount of flow and does not have any outgoing edges.

This concept will be crucial in solving our MFF problem, as we will see in section II-E.

D. Flow Network generation

To achieve our main objective of finding feasible paths for MFF, we first transform the physical space into a flow network. The process of this transformation will be discussed in detail in this section. To avoid inter-UAV collisions, we create a network where intersections between the paths are not possible.

Initially, we take the start and goal positions of the UAVs and create a minimum bounding box that covers the smallest volume possible. We then divide the (3D) box into cubic cells with dimensions of d x d x d meters. We choose the dimension based on the GPS or localization tolerance.

Algorithm 1 Finding Bounding Box

```
1: function FINDBOUNDINGBOX(Positions)
          x_{min} \leftarrow \infty
3:
          y_{min} \leftarrow \infty
 4:
          z_{min} \leftarrow \infty
 5:
          x_{max} \leftarrow 0
 6:
          y_{max} \leftarrow 0
7:
          z_{max} \leftarrow 0
          for point \leftarrow points do
8:
9:
               x_{min} \leftarrow \text{MINIMUM}(x_{min}, point_x)
10:
               x_{max} \leftarrow \text{MAXIMUM}(x_{min}, point_x)
               y_{min} \leftarrow \text{MINIMUM}(y_{min}, point_y)
11:
               y_{max} \leftarrow \text{MAXIMUM}(y_{min}, point_u)
12:
               z_{min} \leftarrow \text{MINIMUM}(z_{min}, point_z)
13:
               z_{max} \leftarrow \text{MAXIMUM}(z_{min}, point_z)
14:
15:
          end for
          return \{x_{max} - x_{min}, y_{max} - y_{min}, z_{max} - z_{min}\}
16:
17: end function
```

Algorithm 2 Sub Dividing the Box into Grid

```
1: function SUBDIVIDEBOXINTOGRID(BoxSize, size)
2: X \leftarrow BoxSize_x/size
3: Y \leftarrow BoxSize_y/size
4: Z \leftarrow BoxSize_z/size
5: return [X, Y, Z]
6: end function
```

Secondly, we further process the resulting grid to take into account static obstacles, free spaces, and valid spaces. After that, we are able to generate a Space Graph (G_s) , shown in Fig. 1. G_s is an undirected weighted graph where the nodes of the graph correspond to the cells in the grid and the edges between any two nodes, n_a and n_b are the paths available to the UAVs from n_a to n_b and vice-versa. The weight of the edge, in most cases, is the Manhattan distance between their

NodesEdges

corresponding grid cells. If, however, the movement is vertical, the cost is H times the normal Manhattan distance. This is to discourage the UAVs from taking unnecessary vertical paths. If a cell in the grid contains a static obstacle, there will be no edges to that node and thus the UAVs will not be able to move into that node. Let us define nodes n_{si} as being nodes that contain our UAVs' starting positions, and n_{ti} as being the nodes that contain our goal positions.

Algorithm 3 Creating the Space Graph

```
1: function CreateSpaceGraph(Grid\overline{Size})
 2:
         N \leftarrow \varnothing
         E \leftarrow \varnothing
 3.
         H \leftarrow 5
                               ▶ This is the vertical movement cost
 4:
     multiplier
         directions \leftarrow \varnothing
 5.
         directions \leftarrow directions \cup \{\{1,0,0\}\}\
 6:
         directions \leftarrow directions \cup \{\{-1,0,0\}\}
 7:
         directions \leftarrow directions \cup \{\{0,1,0\}\}\
 8:
         directions \leftarrow directions \cup \{\{0, -1, 0\}\}
 9:
         directions \leftarrow directions \cup \{\{0,0,1\}\}
10:
11:
         directions \leftarrow directions \cup \{\{0,0,-1\}\}
         for x \leftarrow [0..GridSize[0]] do
12:
              for y \leftarrow [0..GridSize[1]] do
13:
                   for z \leftarrow [0..GridSize[2]] do
14:
                        N = N \cup \text{GETNODE}([x, y, z])
15:
16:
                   end for
              end for
17:
         end for
18:
19.
         for x \leftarrow [0..GridSize[0]] do
20:
              for y \leftarrow [0..GridSize[1]] do
21:
22:
                   for z \leftarrow [0..GridSize[2]] do
                        for dir \leftarrow directions do
23:
                             N_a \leftarrow \text{GETNODE}([x, yz])
24:
                             N_b \leftarrow \text{GETNODE}([x, yz] + dir)
25:
                             mod \leftarrow dir
26:
                            mod[2] \leftarrow mod[2] \cdot H
27:
                             D \leftarrow MANHATTANDISTANCE(mod)
28:
                             E \leftarrow E \cup \{\{N_a, N_b, D\}\}
29:
                        end for
30:
                   end for
31:
              end for
32:
         end for
33:
34:
         G_s \leftarrow (N, E)
         return G_s
35:
36: end function
37:
```

Thirdly, we generate another graph, the State Graph (G_x) , as a directed weighted graph. For each node in G_s , let there be two types of nodes in G_x called an entrance node and an exit node. We then define a directed edge from the entrance node to the exit node. For the edge between nodes n_a and n_b in G_s , we define two new directed edges from n_{ax} to n_{be} and from n_{bx} to n_{ae} , shown in Fig. 2, where x means exit and e

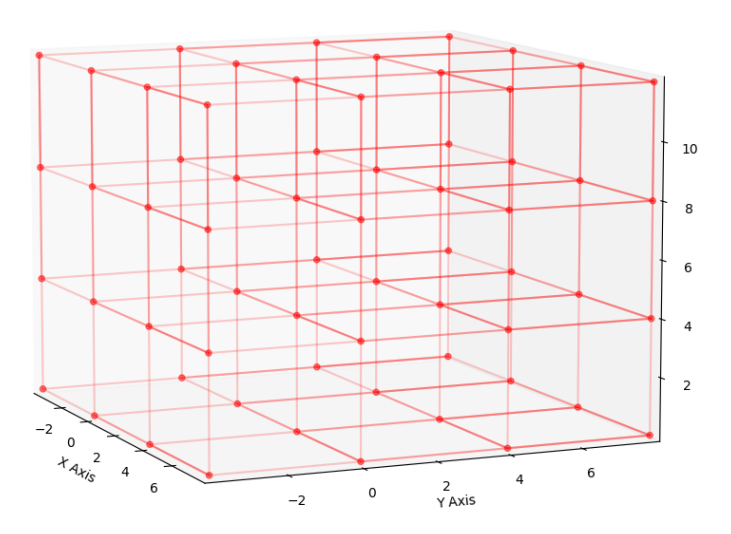


Fig. 1. Space Graph showing the nodes and edges

means entrance. One of the paths will automatically become illegal, as will be shown later in the implementation of the Ford-Fulkerson algorithm.

Finally, we set two abstract nodes, which do not correspond to any physical space, a *virtual source node*, s_v , and a *virtual sink node*, t_v , and we set a directed edge from the virtual source to each of the entrances of the starting nodes, n_{sie} and a directed edge for each of the exits of the goal nodes, n_{tix} to the *virtual sink*. We set all the edges to have a capacity of 1, where the capacity of an edge is the number of times a UAV is able to move through that edge. We claim that the solution to the Maximum Flow Problem of this G_x (flow network) will correspond to our collision-free paths in the grid space.

E. Maximum Flow Problem and Ford Fulkerson Algorithm

The maximum flow problem asks a very simple question. Given a flow network, what is the maximum amount of flow that can be passed through the network from the *source* node to the *sink* node? In our case, we need to find how many UAVs we can send through the network so that no two UAVs occupy the same node at any instant.

We can interpret the path of a UAV as corresponding to a flow from the source node to the sink node. We guarantee that no UAV can occupy the same node concurrently by setting the capacity of the edges to 1. This is especially relevant on the inner edges between the entry and exit nodes, represented in Fig. 2 by the blue-yellow lines. As long as a UAV at any point moves to that node's corresponding grid cell, the flow in the inner edge is set to be 1, which fulfills its capacity. By doing so, any possibility of collision is avoided. An explanation of this is given in Section II-F.

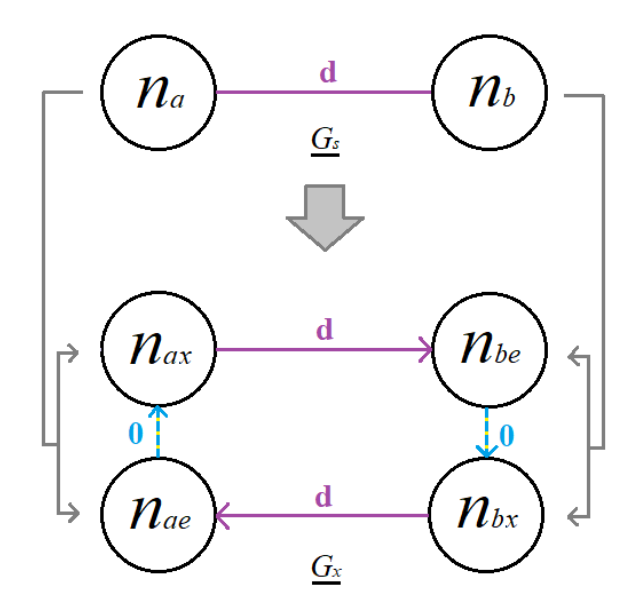
Conversion from G_s to G_x

1: **function** CreateS TateGraph(G_s , starts, goals) $N \leftarrow \varnothing$ 2: $E \leftarrow \varnothing$ 3: $C \leftarrow \varnothing$ 4: for $edge \leftarrow G_s$ do 5: $n_a, n_b, d \leftarrow edge$ 6: $n_{ae} \leftarrow \text{EntryNode}(n_a)$ 7: $n_{ax} \leftarrow \text{EXITNODE}(n_a)$ 8: $n_{be} \leftarrow \text{EntryNode}(n_b)$ 9. $n_{bx} \leftarrow \text{EXITNODE}(n_b)$ 10: $N \leftarrow N \cup \{n_{ae}, n_{ax}, n_{be}, n_{bx}\}$ 11: 12: $NewEdges \leftarrow \{$ $\{n_{ae}, n_{ax}, 0\},\$ 13: $\{n_{be}, n_{bx}, 0\},$ 14: $\{n_{ax}, n_{be}, d\},$ 15: $\{n_{bx}, n_{ae}, d\}$ 16: 17: 18: $E \leftarrow E \cup NewEdges$ end for 19: $N \leftarrow N \cup \{s, t\}$ 20: $\textbf{for } node \leftarrow starts \textbf{ do}$ 21: $entry \leftarrow \text{EntryNode}(node)$ 22: 23: $E \leftarrow E \cup \{\{s, entry, 0\}\}$ end for 24: for $node \leftarrow goals$ do 25: $exit \leftarrow ExitNode(node)$ 26: $E \leftarrow E \cup \{\{exit, t, 0\}\}$ 27: 28: end for 29: for $edge \leftarrow E$ do $C(edge) \leftarrow 1$ ▷ One UAV can cross one path 30: end for 31: $G_x \leftarrow (N, E, C)$ 32: return G_r 33: 34: end function

Algorithm 4 Create State Graph

Algorithm 5 Whole Solution to MFF

```
1: procedure MFFSOLVER
       Start \leftarrow the starting positions of the UAVs
2:
       Goal \leftarrow the goal locations of the UAVs
3:
       MinBox \leftarrow FINDBOUNDINGBOX(Start + Goal)
4:
       Grid \leftarrow SubDivideBoxIntoGrid(MinBox)
5:
       G_s \leftarrow \mathsf{CREATESPACEGRAPH}(Grid)
6:
       G_x \leftarrow \mathsf{CREATESTATEGRAPH}(G_s)
7:
       Paths \leftarrow FordFulkerSon(G_x)
8:
10: end procedure
```



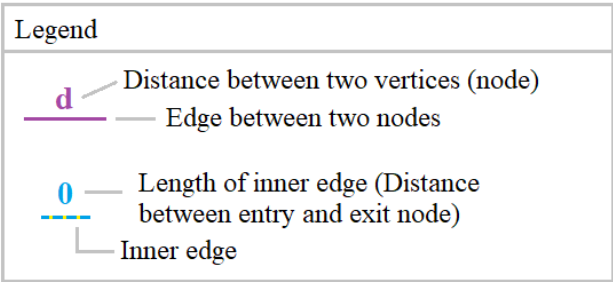


Fig. 2. A pair of connected nodes in G_s getting converted into Two pairs of nodes and interconnected edges in G_x

In G_x , the maximum flow will always correspond to the number of total UAVs if and only if each UAV can pass through the network using a set of edges from the source to the sink in which the total flow is 1. In that case, there exists a set of collision-free paths for each UAV. The real paths of the UAVs will start from the node next to the sources and end just before the sinks, which in our case are conveniently the starting nodes and the ending nodes.

We use the Ford Fulkerson Algorithm [18] to find a solution to the maximum flow problem in G_x . The algorithm depends upon three important ideas of residual networks, augmenting paths, and cuts [19]. The residual graph, G_f , is important for augmenting paths to find maximum flow.

 $Paths \leftarrow \text{FORDFULKERSON}(G_x) \\ WayPoints \leftarrow \text{SAMPLEPOINTS}(Paths, \#Waypoints) \\ \textbf{I procedure} \\ \\ \textbf{I procedure} \\ \\ \textbf{I maximum flow an edge can handle is the capacity of that edge, } C(e). The residual capacity of an edge, } R(e) is the maximum flow an edge can handle in the residual graph, } G_f, \text{ therefore, for any edge, } R(e) = C(e) - f(e).$ It must also be assumed that the flow coming into a node must equal the flow out of a node, with the exception of the

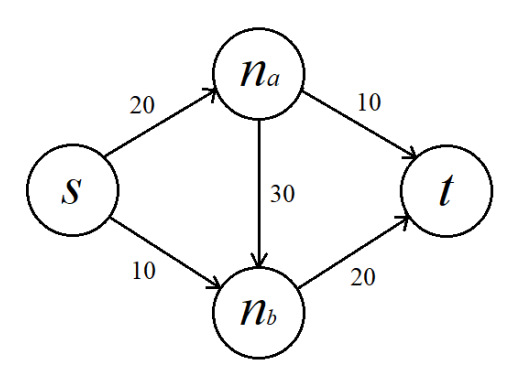
source and sink nodes. Thus, for any node $n \in V - \{s, t\}$:

$$\sum_{e \in E: n \in e} f(e) = 0 \tag{1}$$

Therefore, it can be deduced that the flow mapping is skew-symmetric. So, for any two nodes $n_a, n_b \in V$:

$$f(\{n_a, n_b\} = -f(\{n_b, n_a\})$$
(2)

Flow Network



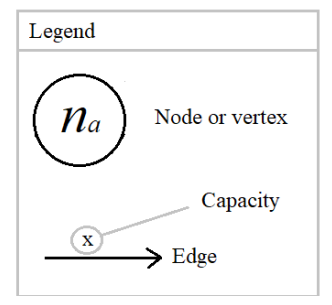


Fig. 3. A flow network, G, with four nodes; s indicates the source, and t indicates the sink.

The procedure of the Ford-Fulkerson Algorithm is as follows:

- 1) If a path from s t is found, apply the bottleneck flow to it. The path in this case is $s \to n_a \to n_b \to t$. (Fig. 3)
- 2) The bottleneck of the path, in this case, is 20, as this is the maximum flow possible in this path. Thus, you have to assign the flow to 20 for all edges in the path. (Fig. 4)
- 3) Build a residual graph G_f as shown in Fig. 5. The edges with zero capacity are not shown as they are not feasible for traversal.
- 4) For a path, P, in the residual graph, that goes from $s \to t$, let the bottleneck, b be the minimum residual capacity on P. The path in this case is $s \to n_b \to n_a \to t$ where b = 10
- 5) Augment the flow using the following equations, shown in Fig. 6
 - If e is a forward edge in P

$$f'(e) = f(e) + b \tag{3}$$

Flow Network with f(e) = 20

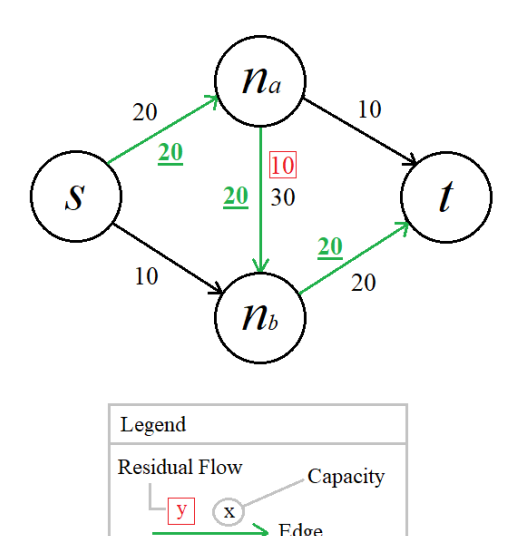


Fig. 4. A directed path and the assigned minimum capacity on that path.

Residual Graph

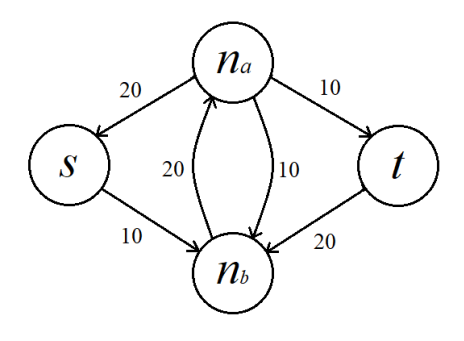


Fig. 5. The residual graph G_f with the new edges

• If e is a backward edge in P

$$f'(e) = f(e) - b \tag{4}$$

6) Repeat steps 1-5 until the maximum flow is found.

Note that there must be an $s \to t$ path in the residual graph for the algorithm to work. As shown in Fig. 7, there is no path; hence the maximum flow is zero.

F. Conflict resolution using the Ford-Fulkerson Algorithm

The Ford-Fulkerson algorithm simply augments the path so that the path found in Bellman-Ford is always *feasible*, which in our case means collision-free. The algorithm also ensures the minimum cost is maintained. The complete proof of the algorithm is outside the scope of this paper.

We can, however, see an example of how the algorithm works in a small subset of the graph. In Fig. 8, we can see

Fig. 6. Final flow network with the augmented flow

2nd Residual Graph

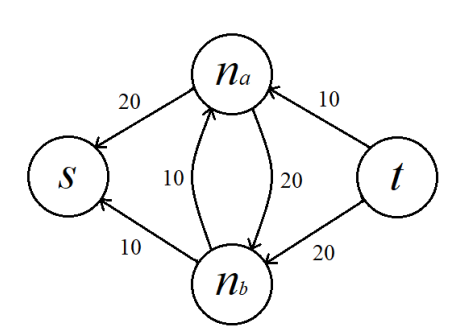


Fig. 7. Final flow network with the augmented flow

if the green path is chosen first, then the red path cannot be chosen, as the two paths will definitely intersect. However, the flow through the red path seems to be zero at first. That is why we need to consider the internal edges between the entry and the exit of the nodes. The capacity of that internal edge has already been fulfilled as one UAV has chosen to pass through that edge. Thus, in actuality, the red path has a bottleneck of zero. Hence, no future UAVs can pass through it, and collision is avoided. A simple solution of such flow network is shown in Fig. 9.

III. EXPERIMENTAL SETUP

A. Simulations

Before actual flights, we generated our planned paths and visualized them with different tools to ensure that our method for MFF actually works. The simulations were conducted on a computer with an 8th gen Intel Core i7 processor and 16GB of RAM. We used the Matplotlib library on Python 3.7 to visualize the patterns. The patterns were chosen in such a way that the collision-avoiding aspect of our algorithm is highlighted.

Conflict resolution in a Flow Network

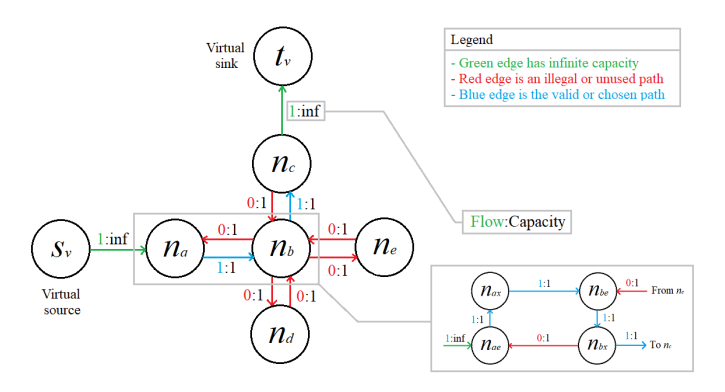


Fig. 8. Conflict resolution in the Flow Network

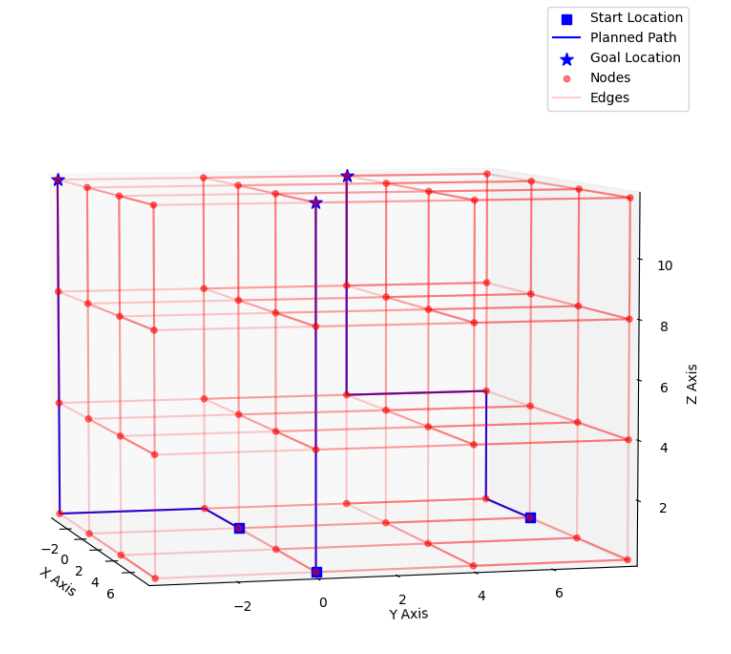


Fig. 9. G_x with a planned path for a certain formation

B. Physical Experiment

Making a quadcopter fly necessitates precise coordination of the motors. Dedicated flight controller hardware is typically used for this. The quadcopters in this work use a Pixhawk flight controller that has been flashed with Arducopter firmware. As the source codes and toolings of the Arducopter firmware are publicly available, it is a popular choice for hobbyists and research UAVs.

In this arrangement, all the quadcopters are connected to a high-gain WiFi access point. The controlling computer and all of the quadcopters are connected to the same local area network. Most commercial WiFi routers come with a 255.255.255.0 (/24) subnet mask set. This means that at most 253 quadcopters and 1 controlling computer can be linked. But this can be configured to have a /23 or lower mask to allow more quadcopters on the network.

Arducopter's "GUIDED" mode accepts commands from

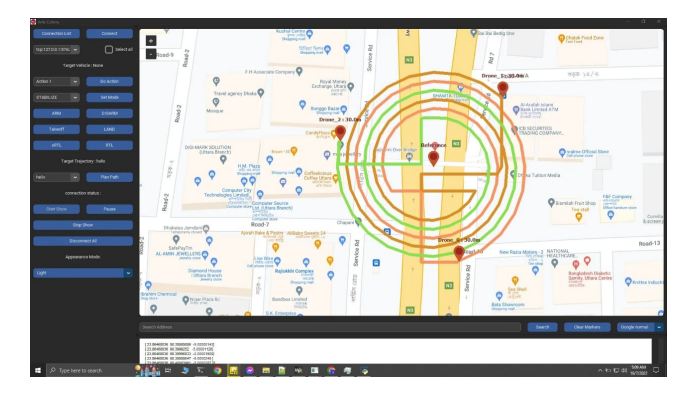


Fig. 10. Our own ground control application running the simulation of the physical experiment.

a remote controller or from a computer with a dedicated telemetry device. The flight controller can additionally take Mavlink [20] messages using its serial communication port. In this setup, Mavlink messages are sent to the flight controller using a wifi link and do not use any dedicated telemetry device. For MFF, the controlling computer sends necessary commands to the quadcopter's companion computer. The term "companion computer" refers to a computer attached to the quadcopter unit itself, often a single-board computer (SBC) like the Raspberry Pi or Nvidia Jetson. The Raspberry Pi runs "Mavproxy" software, which has the ability to forward Mavlink messages received from the controlling computer to the flight controller through a USB connection.

As for the mavlink messages, we use the dronekit library to send the Mavlink messages to the Raspberry Pi. These Mavlink messages are forwarded using the Mavproxy service on the Raspberry Pi [20]. Then we set the quadcopter to "GUIDED" mode and send the coordinates that they should go to. The Pixhawk manages the rest of the process of actually moving the quadcopter to that point.

The same computer that was used for the simulation of patterns was used to simulate the physical experiment as well. It was done in our own proprietary ground control application, shown in Fig. 10.

IV. RESULTS AND DISCUSSIONS

A. Simulations

Figs. 12, 11, and 13 shows our simulation of several formations using UAVs. The red lines correspond to the paths taken by each of the UAVs. Although not clearly visible here in a two-dimensional plane, the paths do not intersect or overlap at any point and are void of collisions. As the complexity of the pattern increases, so do the number of UAVs needed for it. The number of nodes corresponds to the total volume of the grid. The computation time differs with different patterns. The 2D shape formations were computed within 2.5 minutes and the more complex, collision-prone 3D shapes took less than 5 minutes (See Table I). The larger the number of connections, the longer the computation time. This is because our method has to first find a longer path and then resolve a greater number

TABLE I
SIMULATIONS OF MULTIFARIOUS FORMATIONS AND THEIR RESPECTIVE
COMPUTATION TIMES

Pattern	Number of UAVs	Nodes	Edges	Computation Time (s)
"ANTS"	51	86940	254171	167.5
Smiley Face	44	101520	297982	148.5
Cube	64	146412	430500	299.4

of conflicts to find collision-free paths. It has to be noted that the computation time has a larger correlation with the size of the grid than the number of UAVs.

B. Physical test

We implemented our algorithm and conducted successful real-life flight tests for MFF. In the experiment, quadcopters are first placed on a grid-like pattern on the XY plane. The starting location data is provided by the onboard GPS of the quadcopters. The median position of quadcopters is used as a local reference for coordinate transformation. The position data is converted from the Latitude, Longitude, and Altitude (LLA) geographic coordinate system to the local XYZ cartesian coordinate system.

After the conversion of the reference frame, a "pattern" is generated in the local frame. The initial location of all the quadcopters is used as a starting location, and points on the generated patterns are considered the goal locations.

Upon completion of path planning, a waypoint on each path was sent as a target location to the appropriate quadcopters in the formation. The above-mentioned step was followed until all the quadcopters had reached their destination.

The whole experiment was first conducted in our ground control application in order to check if our workflow is compatible with the Arducopter firmware. Upon completion of the simulation of the experiment, tests were carried out at the flying field, shown in Fig. 14. Three quadcopters completed their task to stay in formation and return without any collision. Fig. 15 shows the quadcopters in mid-flight.

As a note, if a quadcopter lost connection or went rogue, it would come back using Smart Return To Launch (SRTL). In that case, the quadcopter just traverses the same path back that it used to go to its final known location. An unintended advantage of this policy is that even in the case of multiple quadcopters failing, the path followed back will always be collision-free.

V. CONCLUSION AND FUTURE WORKS

In this paper, we have implemented a method of utilizing graph-based flow networks to devise a method for MFF. It has three main parts: first, it generates a flow network graph from physical GPS coordinates; second, it uses the Bellman-Ford algorithm to find the path with the shortest distance; and finally, it employs the Ford-Fulkerson Method to find collision-free paths. We can ensure that it generates paths in which UAVs can safely fly in close proximity to one another. It was validated by several software-in-the-loop (SITL) simulations

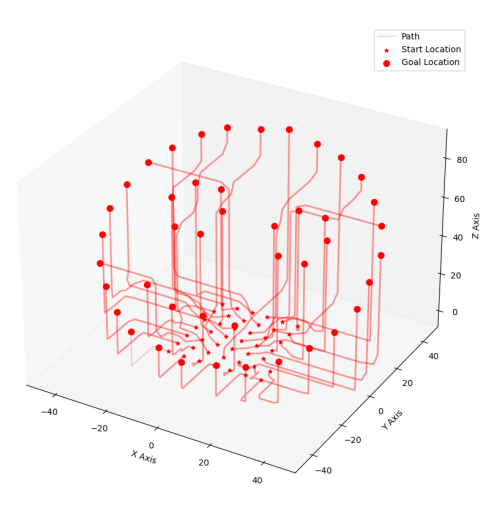


Fig. 11. 'Smiley Face' formation in a 45-degree slant using 41 UAVs. Starting and goal positions are represented using stars and dots, respectively.

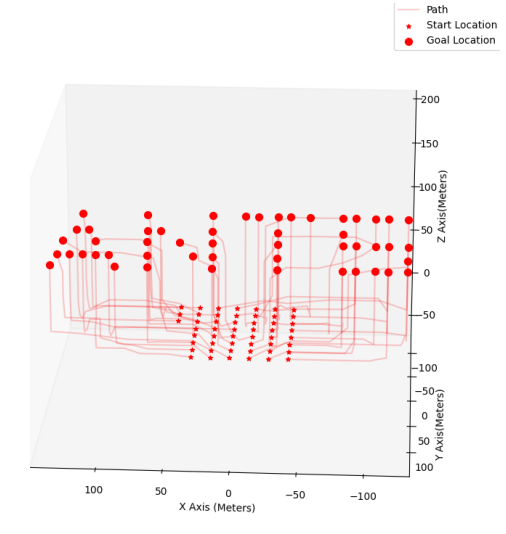


Fig. 12. 'ANTS' formation using 51 UAVs

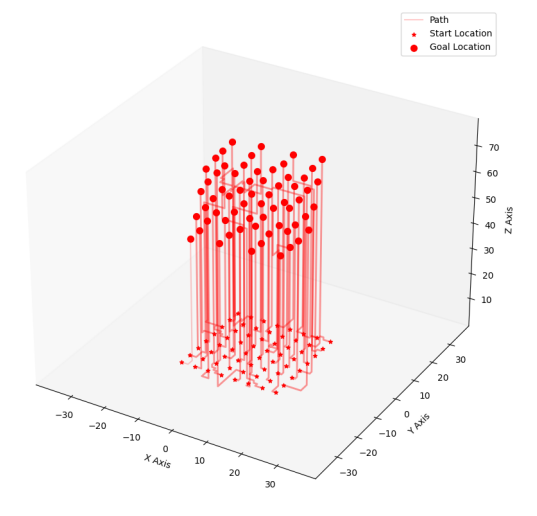


Fig. 13. 'Cube' formation using 64 UAVs

of up to 64 UAVs, as well as by conducting multiple outdoor flight tests in predefined formations of 3 quadcopters. Fast computation times for finding the paths for MFF demonstrated that our method is efficient and reliable.

Future improvements to this work could be in terms of improvement in localization techniques, as GPS-based localization can be expensive and imprecise at times. We may also incorporate a trajectory planner in future to allow for a more seamless and coordinated movement of UAVs.

Furthermore, the addition of velocity control will enable us to perform direct comparisons with current methods of MFF. This is due to the fact that a time-based parameter is typically used in path or trajectory planning literature as a performance indicator.



Fig. 14. The quadcopters (UAVs) in their starting positions.



Fig. 15. Quadcopters in operation, following the paths generated by the MFF Solver.

REFERENCES

- U. R. Mogili and B. Deepak, "Review on application of drone systems in precision agriculture," *Procedia computer science*, vol. 133, pp. 502–509, 2018.
- [2] N. Hallermann and G. Morgenthal, "Visual inspection strategies for large bridges using unmanned aerial vehicles (uav)," in *Proc. of 7th IABMAS, International Conference on Bridge Maintenance, Safety and Management*, 2014, pp. 661–667.
- [3] N. Metni and T. Hamel, "A uav for bridge inspection: Visual servoing control law with orientation limits," *Automation in construction*, vol. 17, no. 1, pp. 3–10, 2007.

- [4] S. J. Kim, Y. Jeong, S. Park, K. Ryu, and G. Oh, "A survey of drone use for entertainment and avr (augmented and virtual reality)," in *Augmented reality and virtual reality*, Springer, 2018, pp. 339–352.
- [5] Y. Wang, P. Bai, X. Liang, W. Wang, J. Zhang, and Q. Fu, "Reconnaissance mission conducted by uav swarms based on distributed pso path planning algorithms," *IEEE Access*, vol. 7, pp. 105 086–105 099, 2019.
- [6] S. Huang, R. S. H. Teo, and K. K. Tan, "Collision avoidance of multi unmanned aerial vehicles: A review," *Annual Reviews* in Control, vol. 48, pp. 147–164, 2019.
- [7] Á. Madridano, A. Al-Kaff, D. Martín, and A. de la Escalera, "Trajectory planning for multi-robot systems: Methods and applications," *Expert Systems with Applications*, vol. 173, p. 114 660, 2021.
- [8] C. Bentes and O. Saotome, "Dynamic swarm formation with potential fields and a* path planning in 3d environment," in 2012 Brazilian Robotics Symposium and Latin American Robotics Symposium, IEEE, 2012, pp. 74–78.
- [9] M. Čáp, P. Novák, J. Vokřínek, and M. Pěchouček, "Multiagent rrt*: Sampling-based cooperative pathfinding," arXiv preprint arXiv:1302.2828, 2013.
- [10] J.-H. Son, H.-S. Ahn, and J. Cha, "Lennard-jones potential field-based swarm systems for aggregation and obstacle avoidance," in 2017 17th International Conference on Control, Automation and Systems (ICCAS), IEEE, 2017, pp. 1068–1072.
- [11] X. Ma, Z. Jiao, Z. Wang, and D. Panagou, "Decentralized prioritized motion planning for multiple autonomous uavs in 3d polygonal obstacle environments," in 2016 International Conference on Unmanned Aircraft Systems (ICUAS), IEEE, 2016, pp. 292–300.
- [12] B. López, J. Muñoz, F. Quevedo, C. A. Monje, S. Garrido, and L. E. Moreno, "Path planning and collision risk management strategy for multi-uav systems in 3d environments," *Sensors*, vol. 21, no. 13, p. 4414, 2021.
- [13] Q. Li, F. Gama, A. Ribeiro, and A. Prorok, "Graph neural networks for decentralized multi-robot path planning," in 2020 IEEE/RSJ International Conference on Intelligent Robots and Systems (IROS), IEEE, 2020, pp. 11785–11792.
- [14] Á. Madridano, A. Al-Kaff, D. Martín, and A. de la Escalera, "3d trajectory planning method for uavs swarm in building emergencies," *Sensors*, vol. 20, no. 3, p. 642, 2020.
- [15] J. Yu and S. M. LaValle, "Multi-agent path planning and network flow," in *Algorithmic foundations of robotics X*, Springer, 2013, pp. 157–173.
- [16] J. Yu and S. M. LaValle, "Planning optimal paths for multiple robots on graphs," in 2013 IEEE International Conference on Robotics and Automation, IEEE, 2013, pp. 3612–3617.
- [17] R. J. Vanderbei et al., Linear programming. Springer, 2020.
- [18] L. R. Ford and D. R. Fulkerson, "Maximal flow through a network," *Canadian journal of Mathematics*, vol. 8, pp. 399– 404, 1956.
- [19] T. H. Cormen, C. E. Leiserson, R. L. Rivest, and C. Stein, Introduction to algorithms. MIT press, 2022.
- [20] A. Koubâa, A. Allouch, M. Alajlan, Y. Javed, A. Belghith, and M. Khalgui, "Micro air vehicle link (mavlink) in a nutshell: A survey," *IEEE Access*, vol. 7, pp. 87 658–87 680, 2019.